International Journal of Research Studies on Environment, Earth, and Allied Sciences (IJRSEAS)
| *Volume-3 Issue-2* | *April-2026* | *ISSN: 3066-0637* | *Website:* https://eesrd.us

Manuscript ID:
IJRSEAS-2026-030227

OPEN ACCESS

Quick Response Code:

Website: https://eesrd.us

DOI: 10.5281/zenodo.21291242

DOI Link:
https://doi.org/10.5281/zenodo.21291242

Volume: 3

Issue: 2

Pp. 137-150

Month: April

Year: 2026

E-ISSN: 3066-0637

Submitted: 10 Mar. 2026

Revised: 20 Mar. 2026

Accepted: 12 Apr. 2026

Published: 30 Apr. 2026

Address for correspondence:
Akshay Patil
Research Scholar, Department of Chemistry, Sandip University, Nashik, Maharashtra, India
Email:
akshay06121991@gmail.com

How to cite this article:
Patil, A.& Ghosh, B. (2026). Preparation and Structural Characterization of 5% Ag doped ZrO_2 Heterogeneous Nano catalyst via Wet Impregnation Method. International Journal of Research Studies on Environment, Earth, and Allied Sciences, 3(2), 137–150.
https://doi.org/10.5281/zenodo.21291242

Preparation and Structural Characterization of 5% Ag doped ZrO_2 Heterogeneous Nano catalyst via Wet Impregnation Method

Akshay Patil[1], Dr. Brijadulal Ghosh[2]
[1]Research Scholar, Department of Chemistry, Sandip University, Nashik, Maharashtra, India
[2]Assistant Professor, Department of Chemistry, Sandip University, Nashik, Maharashtra, India

Abstract

The development of supported noble metal nanocatalysts has attracted significant attention due to their wide applicability in heterogeneous catalysis. In the present study, a 5 wt% silver-doped zirconia (Ag/ZrO2) heterogeneous nanocatalyst was successfully prepared via a controlled wet impregnation method followed by calcination. Zirconium dioxide (ZrO2) was used as a thermally stable support owing to its high surface area, amphoteric nature, and strong metal–support interaction properties. Silver nanoparticles were deposited onto the ZrO2 surface using silver nitrate as a precursor. The synthesized nano catalyst was structurally characterized using X-ray diffraction (XRD), Fourier transform infrared spectroscopy (FTIR), scanning electron microscopy (SEM), transmission electron microscopy (TEM), energy-dispersive X-ray analysis (EDAX), UV–Visible diffuse reflectance spectroscopy (UV–Vis DRS), and Brunauer–Emmett–Teller (BET) surface area analysis. XRD results confirmed the crystalline phases of ZrO2 and the successful incorporation of metallic silver. SEM and TEM analysis revealed well-dispersed Ag nanoparticles over the ZrO2 surface. EDAX confirmed approximately 5 wt% silver loading. UV–Vis DRS showed a surface plasmon resonance band characteristic of silver nanoparticles. The developed material demonstrates desirable structural and physicochemical properties suitable for heterogeneous catalytic applications.

Keywords: *Silver nanoparticles, Zirconia, Wet impregnation, Heterogeneous nano catalyst, Structural characterization*

Introduction

Heterogeneous catalysis represents one of the most critical technological pillars underpinning modern chemical manufacturing, environmental protection, and sustainable energy systems. It is estimated that over 80% of chemical processes involve at least one catalytic step, highlighting the economic and societal importance of catalyst design and optimization. The performance of heterogeneous catalysts is fundamentally governed by surface-mediated reactions occurring at solid–gas or solid–liquid interfaces, where adsorption, activation, transformation, and desorption of reactant molecules take place. In recent decades, the transition from bulk catalytic materials to nanoscale systems has revolutionized the field, as nanostructured catalysts offer dramatically increased surface atom fractions, tunable electronic properties, and enhanced interfacial phenomena compared to their bulk counterparts [1,2]. At the nanoscale, the catalytic behavior becomes highly sensitive to particle size, morphology, crystallographic orientation, and metal–support interactions, making structural control during synthesis a central requirement for rational catalyst design [17,30,35].

The conceptual framework of modern supported metal catalysis is built upon the understanding that catalytic activity does not solely arise from the intrinsic properties of the active metal but rather from a complex synergy between the metal nanoparticles and the support material. This synergy encompasses geometric effects (particle size and shape), electronic effects (charge transfer and band structure modification), and chemical effects (interfacial defect formation and adsorption energetics). The electronic metal–support interaction can modify the density of states near the Fermi level of the metal, thereby influencing adsorption strength of reactants and intermediates according to d-band center theory [17,30]. Moreover, nanoscale particles exhibit quantum confinement effects and increased fractions of low-coordination atoms, which can significantly alter catalytic pathways and turnover frequencies [35,37]. Therefore, achieving controlled dispersion of active metal nanoparticles over a stable oxide support remains a primary objective in heterogeneous catalyst development. Zirconium dioxide (ZrO_2) has emerged as a highly versatile oxide support due to its exceptional thermal stability, amphoteric surface properties, and structural polymorphism.

Unlike silica, which is largely inert and weakly acidic, zirconia possesses both Lewis acidic Zr^{4+} centers and basic O^{2-} sites, enabling it to participate actively in bifunctional catalytic mechanisms [13,39]. The amphoteric character of zirconia arises from its ability to accept and donate electron density, making it suitable for acid–base catalysis, redox transformations, and coupling reactions. Structurally, zirconia exhibits three primary crystalline polymorphs: monoclinic (thermodynamically stable at room temperature), tetragonal (stable at elevated temperatures or nanoscale dimensions), and cubic (stable at high temperatures or when doped with stabilizers). The tetragonal phase, often stabilized in nanoscale systems due to surface energy considerations, is associated with enhanced oxygen mobility and defect density, which are advantageous for oxidation reactions [5,6]. The ability to manipulate zirconia phase composition through calcination and synthesis parameters allows tuning of its catalytic and interfacial properties.

The surface chemistry of zirconia further contributes to its suitability as a catalyst support. The presence of terminal and bridging hydroxyl groups formed through interaction with atmospheric moisture creates active anchoring sites for metal precursor ions during synthesis [36]. These hydroxyl groups facilitate adsorption of metal cations through electrostatic interactions or ligand exchange mechanisms, ensuring initial dispersion prior to thermal treatment. Additionally, zirconia can accommodate oxygen vacancies within its lattice, particularly under reducing or high-temperature conditions. These vacancies act as electron-rich defect sites capable of stabilizing metal nanoparticles and enhancing interfacial redox reactions. Oxygen vacancies also influence adsorption and activation of molecular oxygen, thereby contributing to catalytic oxidation pathways. Consequently, zirconia is not merely a passive support but an active participant in interfacial catalytic chemistry.

Silver, as a noble metal, possesses a unique electronic structure characterized by a filled d-band and relatively weak binding strength toward oxygenated intermediates. This moderate adsorption energy profile often translates into superior selectivity in partial oxidation reactions compared to more strongly adsorbing metals such as platinum or palladium [16,34]. Industrially, silver catalysts are extensively employed in ethylene epoxidation, formaldehyde production from methanol, and selective oxidation of hydrocarbons. The catalytic properties of silver are highly structure-sensitive, meaning that particle size, shape, and oxidation state significantly influence activity and selectivity [25,26]. For example, nanoscale silver particles with diameters below 20 nm exhibit increased proportions of edge and corner atoms, which serve as highly reactive sites for adsorption and activation of oxygen molecules. At the nanoscale, silver nanoparticles exhibit a phenomenon known as surface plasmon resonance (SPR), which arises from the collective oscillation of conduction electrons under electromagnetic excitation. The SPR band, typically observed in the 400–450 nm region in UV–Visible spectroscopy, provides valuable information regarding particle size distribution, morphology, and dielectric environment [25,29]. Shifts in SPR peak position or intensity may indicate changes in nanoparticle aggregation, oxidation state, or interfacial interactions with the support. Thus, spectroscopic analysis of SPR features serves as an important diagnostic tool for confirming successful formation of metallic silver nanoparticles following calcination. The optical properties of silver nanoparticles further underscore the importance of controlling nucleation and growth processes during synthesis.

When silver nanoparticles are dispersed over zirconia support, interfacial phenomena become central to catalytic performance. The concept of strong metal–support interaction (SMSI) describes the electronic and structural modifications occurring at the metal–oxide interface, often resulting in enhanced stability and modified catalytic behavior [17,31]. In Ag/ZrO_2 systems, partial electron transfer between silver nanoparticles and oxygen-deficient zirconia may occur, influencing adsorption strength of oxygen and other reactants. The interfacial region may facilitate the formation of reactive oxygen species such as superoxide or peroxide intermediates, which play key roles in oxidation reactions [3,4]. Moreover, the crystallographic phase of zirconia influences metal anchoring strength and dispersion, with tetragonal zirconia often providing improved stabilization due to higher defect density and surface energy [6]. These findings highlight the necessity of precise control over preparation parameters to maximize metal dispersion and interfacial contact area.

Among various preparation methods for supported metal catalysts—including sol–gel synthesis, deposition–precipitation, hydrothermal methods, and chemical vapor deposition—wet impregnation remains one of the most practical and industrially scalable techniques [2,12,33]. The wet impregnation process involves dissolving a metal precursor (commonly silver nitrate in the case of Ag catalysts) in a suitable solvent and contacting the solution with the porous support material. Metal ions diffuse into the pore network and adsorb onto surface hydroxyl groups. Subsequent drying removes the solvent, while calcination decomposes the precursor to yield metallic or oxide nanoparticles anchored to the support surface [37]. The simplicity of this method enables accurate control over metal loading by adjusting precursor concentration, making it particularly suitable for preparing catalysts with defined compositions such as 5 wt% Ag/ZrO_2. However, the physicochemical processes occurring during drying and calcination are highly complex. During solvent evaporation, capillary forces can induce migration of dissolved precursor species toward pore mouths, potentially leading to non-uniform metal distribution if drying conditions are not carefully controlled [2,48]. Calcination temperature plays a critical role in determining final nanoparticle size, as excessively high temperatures may promote sintering through Ostwald ripening or particle coalescence [33]. Conversely, insufficient thermal treatment may result in incomplete precursor decomposition, leaving residual nitrate species that could affect catalytic performance. Therefore, optimization of impregnation concentration, drying kinetics, heating rate, and calcination temperature is essential for achieving homogeneous dispersion of nanoscale silver particles over zirconia support.

The selection of 5 wt% silver loading represents a strategically balanced composition for structural and catalytic studies. At lower loadings, isolated metal clusters may not provide sufficient active surface density for

cooperative surface reactions, whereas higher loadings increase the probability of nanoparticle agglomeration and reduced dispersion [7,13]. A 5 wt% loading ensures measurable crystalline reflections in X-ray diffraction while maintaining nanoscale particle size suitable for high catalytic surface area. This composition also maximizes interfacial contact between silver nanoparticles and zirconia, enhancing potential SMSI effects and facilitating detailed structural characterization. Comprehensive structural characterization is indispensable for correlating synthesis parameters with catalyst properties. X-ray diffraction (XRD) analysis enables identification of zirconia polymorphs and detection of metallic silver reflections, with peak broadening providing estimates of crystallite size via the Scherrer equation [21]. Fourier transform infrared spectroscopy (FTIR) reveals information regarding surface hydroxyl groups and possible shifts indicative of metal–support coordination [22]. Scanning electron microscopy (SEM) and transmission electron microscopy (TEM) permit direct observation of morphology and nanoparticle dispersion at micro- and nanoscales [23,24]. Energy-dispersive X-ray analysis (EDAX) confirms elemental composition and verifies the targeted silver loading. Brunauer–Emmett–Teller (BET) surface area analysis assesses changes in porosity and surface area following metal deposition [19,20]. UV–Visible diffuse reflectance spectroscopy (DRS) confirms formation of metallic silver nanoparticles via characteristic SPR bands [25,29]. Integration of these techniques enables a multidimensional understanding of structural, morphological, and electronic properties of the synthesized nanocatalyst.

Literature Review:

The development of supported noble metal catalysts has been a central focus in heterogeneous catalysis research for several decades, driven by the need to enhance catalytic efficiency while minimizing noble metal usage. Early investigations into supported catalyst systems established that dispersion of metal nanoparticles over high-surface-area oxides significantly enhances catalytic performance compared to bulk metals due to increased availability of surface-active sites [2,32]. Subsequent advancements in nanoscience revealed that catalytic activity is highly structure-sensitive, with turnover frequencies strongly dependent on particle size, morphology, and metal–support interfacial characteristics [35,37]. These findings laid the foundation for systematic exploration of supported nanocatalysts, including silver-based systems supported on metal oxides such as Al_2O_3, TiO_2, CeO_2, SiO_2, and ZrO_2.

Silver-supported catalysts have historically been studied for selective oxidation processes, particularly ethylene epoxidation, where Ag/Al_2O_3 systems became industrially established. However, research over the past two decades has expanded toward alternative oxide supports to improve dispersion, oxygen activation capability, and resistance to sintering. Among these supports, zirconium dioxide has gained increasing attention due to its amphoteric character and oxygen vacancy formation capability [5,39]. Compared to alumina, zirconia provides stronger metal anchoring sites through coordinatively unsaturated Zr^{4+} centers and surface hydroxyl groups, which facilitate improved nanoparticle stabilization [36]. Studies have demonstrated that zirconia-supported silver catalysts exhibit enhanced redox performance in soot oxidation and hydrocarbon oxidation reactions compared to conventional supports [3,4]. The role of zirconia crystalline phase has been extensively investigated in literature. It has been reported that the tetragonal phase of ZrO_2 often provides superior catalytic performance compared to the monoclinic phase due to higher oxygen mobility and defect density [6]. Guo et al. demonstrated that phase-engineered zirconia significantly influences silver dispersion and catalytic oxidation activity, attributing improved performance to enhanced metal–support electronic interaction [6]. Similarly, Reddy and co-workers highlighted that surface acidity and defect concentration vary among zirconia polymorphs, thereby affecting adsorption energetics of reactants [13]. These studies collectively suggest that structural properties of zirconia must be carefully controlled during synthesis to achieve optimal catalytic behavior.

The phenomenon of strong metal–support interaction (SMSI) has been a recurring theme in studies involving silver supported on reducible oxides. Although SMSI was originally described for systems such as Pt/TiO_2, subsequent research demonstrated that zirconia can also induce electronic perturbations at the metal–oxide interface [17,31]. In Ag/ZrO_2 systems, partial electron transfer between silver nanoparticles and oxygen-deficient zirconia has been proposed to modify the d-band center of silver, thereby influencing adsorption strength of oxygen molecules [30]. Nanba et al. reported that reactive oxygen species generated at the $Ag–ZrO_2$ interface are responsible for enhanced soot oxidation activity at relatively low temperatures [3,4]. These findings underscore the importance of interfacial defect chemistry in determining catalytic performance.

Preparation methodology plays a critical role in determining nanoparticle dispersion and interfacial structure. Among various synthesis techniques, wet impregnation remains widely used due to its operational simplicity and scalability [2,12,33]. Studies comparing impregnation with sol–gel and deposition–precipitation methods have shown that impregnation allows precise control over metal loading but may require careful optimization of drying and calcination parameters to avoid metal agglomeration [2]. During impregnation, metal precursor ions adsorb onto hydroxylated support surfaces, and subsequent calcination induces decomposition and nucleation of metallic nanoparticles. However, migration of precursor species during solvent evaporation can lead to inhomogeneous metal distribution if drying kinetics are not properly controlled [48]. Therefore, the literature emphasizes controlled heating rates and moderate calcination temperatures to minimize sintering effects [33,37].

The influence of metal loading on structural and catalytic properties has been systematically studied. It has been observed that silver loadings below 1 wt% often result in highly dispersed but isolated metal clusters with limited cooperative catalytic activity, whereas loadings above 10 wt% frequently promote particle coalescence and decreased dispersion [7,13]. Several reports suggest that intermediate loadings around 5 wt% provide an optimal

balance between active site density and nanoparticle stabilization, allowing measurable crystalline reflections in XRD while maintaining nanoscale dispersion [33]. This moderate loading enhances interfacial contact area without excessive agglomeration, thereby maximizing potential SMSI effects. Characterization techniques employed in literature further illuminate structural–property relationships in Ag/ZrO_2 systems. X-ray diffraction has been extensively used to monitor zirconia phase stability and detect metallic silver peaks near $2\theta \approx 38°$, 44°, and 64°, corresponding to the (111), (200), and (220) planes of face-centered cubic silver [21]. Broadening of these reflections is often associated with nanoscale particle size. Fourier transform infrared spectroscopy studies have reported shifts in Zr–O–Zr stretching vibrations upon silver loading, suggesting modification of surface hydroxyl environments [22]. Transmission electron microscopy has revealed silver nanoparticle sizes typically ranging from 5–30 nm depending on calcination temperature and loading [23,24]. BET surface area measurements commonly show slight decreases after metal deposition due to partial pore blockage [19,20].

Optical characterization through UV–Vis diffuse reflectance spectroscopy has provided additional evidence of silver nanoparticle formation. The appearance of a characteristic surface plasmon resonance band around 420 nm confirms the presence of metallic Ag^0 species [25,29]. Shifts in SPR peak position have been correlated with changes in particle size and aggregation state. Furthermore, X-ray photoelectron spectroscopy (XPS) studies reported in literature indicate that both metallic Ag^0 and oxidized Ag^+ species may coexist depending on calcination atmosphere and temperature, with the Ag $3d_5/_2$ binding energy serving as a diagnostic indicator of oxidation state [30]. Such spectroscopic insights highlight the importance of controlled thermal treatment in determining final electronic structure. Thermal stability and sintering resistance of Ag/ZrO_2 catalysts have also been addressed in literature. Studies have shown that zirconia supports provide stronger anchoring compared to silica due to higher surface energy and defect density, reducing nanoparticle mobility during high-temperature operation [36]. However, excessive calcination temperatures above 600°C may still induce significant particle growth through Ostwald ripening mechanisms [33]. Therefore, optimization of calcination temperature in the range of 400–500°C is commonly reported to achieve complete precursor decomposition while minimizing sintering [37].

Recent advancements have also explored modifications of zirconia through doping or composite formation to enhance silver stabilization. For example, incorporation of ceria or yttria into zirconia has been reported to increase oxygen vacancy concentration and improve redox properties, thereby influencing silver dispersion and catalytic activity [38]. Nevertheless, undoped zirconia remains an important model system for investigating intrinsic metal–support interactions without additional compositional complexity. Despite extensive research on silver-supported catalysts, the literature reveals variability in synthesis conditions, loading percentages, and calcination protocols, making direct comparison among studies challenging. Many reports focus primarily on catalytic performance without comprehensive structural analysis, while others emphasize characterization without systematic evaluation of preparation parameters. Consequently, there remains a need for controlled synthesis of 5 wt% Ag/ZrO_2 via a standardized wet impregnation approach, followed by detailed structural characterization to establish reproducible structure–property correlations.

In summary, previous investigations have established that zirconia is a thermally stable and electronically interactive support capable of stabilizing silver nanoparticles through defect-mediated anchoring mechanisms. Silver loading, nanoparticle dispersion, zirconia phase composition, and calcination temperature collectively influence structural and electronic characteristics of the catalyst. Wet impregnation remains a practical and scalable preparation method, yet precise control over processing parameters is essential to achieve homogeneous nanoscale dispersion. Building upon these insights, the present work focuses on controlled preparation and systematic structural characterization of 5 wt% Ag-doped ZrO_2 heterogeneous nanocatalyst, aiming to contribute to the deeper understanding of metal–support interactions and nanoparticle stabilization mechanisms in silver-based catalytic systems.

Materials and Methods:

Zirconium dioxide (ZrO_2) nanopowder (analytical grade, ≥99% purity, average particle size <50 nm) was used as the catalyst support. The support was selected due to its high thermal stability, amphoteric surface properties, and ability to stabilize dispersed noble metal nanoparticles through surface hydroxyl interactions.

Silver nitrate ($AgNO_3$, ≥99.9% purity, analytical grade) was employed as the silver precursor because of its high solubility in water, controlled thermal decomposition behavior, and suitability for impregnation techniques.

Distilled deionized water (resistivity ≥18 MΩ·cm) was used as the impregnation solvent to avoid contamination from dissolved ions. Ethanol (analytical grade) was optionally used for final washing to remove weakly physisorbed species and promote rapid solvent evaporation during drying.

All chemicals were used as received without further purification. Prior to use, ZrO_2 support was dried at 120°C for 2 h to remove physiosorbed moisture and ensure reproducible impregnation conditions. Glassware was cleaned with dilute nitric acid and rinsed thoroughly with distilled water to eliminate trace metal contamination.

3.2 Calculation of 5 wt% Silver Loading

The catalyst composition was designed to contain 5 wt% metallic silver relative to the total mass of catalyst. For preparation of 1.0 g of Ag/ZrO_2 catalyst:

Target silver mass:

$$5\% \times 1\ \text{g} = 0.05\ \text{g Ag}$$

Since silver nitrate ($AgNO_3$) was used as precursor, stoichiometric correction was necessary.

Molecular weights:

- Ag = 107.86 g·mol^{-1}
- $AgNO_3$ = 169.87 g·mol^{-1}

Conversion factor:

$$\frac{169.87}{107.86} = 1.57$$

Thus, required $AgNO_3$ mass:

$$0.05 \times 1.57 = 0.0785 \text{ g}$$

Accordingly, 0.078 g of $AgNO_3$ was weighed accurately using an analytical balance (±0.1 mg precision) and impregnated onto 0.95 g of ZrO_2 support to achieve theoretical 5 wt% silver loading.

This stoichiometric calculation ensures accurate control of metal loading, which is critical for reproducibility and structural analysis.

3.3 Preparation of 5 wt% Ag/ZrO_2 Nanocatalyst

The nanocatalyst was synthesized via a controlled wet impregnation technique followed by thermal calcination.

Step 1: Preparation of Silver Precursor Solution

Precisely 0.078 g of $AgNO_3$ was dissolved in 20 mL of distilled water under magnetic stirring at ambient temperature (~25°C). The solution was stirred for 15–20 minutes until complete dissolution and formation of a clear, homogeneous solution.

The aqueous medium ensures full dissociation of $AgNO_3$:

$$AgNO_3 \rightarrow Ag^+ + NO_3^-$$

The pH of the solution was measured (typically between 6–7). Maintaining near-neutral pH prevents premature hydrolysis or precipitation of silver species.

Step 2: Impregnation Process

Pre-dried 0.95 g ZrO_2 nanopowder was gradually added to the $AgNO_3$ solution under continuous magnetic stirring to ensure uniform wetting of the support.

The suspension was stirred for 4 h at room temperature. During this period:

- Ag^+ ions diffuse into the pore structure of ZrO_2
- Electrostatic attraction occurs between Ag^+ and negatively charged surface hydroxyl groups (Zr–OH)
- Ligand exchange interactions may occur

Surface adsorption mechanism:

$$Zr\text{–}OH + Ag^+ \rightarrow Zr\text{–}O\text{–}Ag + H^+$$

The extended stirring time ensures equilibrium adsorption and uniform distribution of silver precursor over the support surface.

Step 3: Drying

The impregnated slurry was transferred to a glass petri dish and dried in a hot air oven at 100°C for 12 h.

Drying serves multiple purposes:

- Removal of solvent
- Immobilization of Ag^+ ions on support surface
- Prevention of excessive precursor mobility

Slow evaporation minimizes capillary-driven migration of silver ions, which could otherwise lead to surface enrichment or inhomogeneous metal distribution.

During drying, silver nitrate crystallizes within the support pores and on the surface.

Step 4: Calcination

The dried precursor material was calcined in a programmable muffle furnace at 450°C for 4 h under ambient air atmosphere.

Heating rate: 5°C·min^{-1}

Soaking time: 4 h

Calcination induces thermal decomposition of silver nitrate through the following steps:

1. Dehydration and melting of $AgNO_3$ (~212°C)
2. Decomposition to silver oxide:

$$2AgNO_3 \rightarrow 2Ag_2O + 2NO_2 + O_2$$

3. Further decomposition of Ag_2O to metallic silver:

$$Ag_2O \rightarrow 2Ag(metallic) + \frac{1}{2}O_2$$

The controlled heating rate prevents rapid gas evolution, which could disrupt particle dispersion. The 450°C temperature is sufficient to ensure complete decomposition while minimizing silver nanoparticle sintering.

After completion, the furnace was allowed to cool naturally to room temperature to avoid thermal shock and structural stress.

The final product appeared as a light grey powder, indicating formation of metallic silver nanoparticles dispersed on zirconia

Characterization Techniques:

1. **Fourier Transform Infrared Spectroscopy (FTIR):**

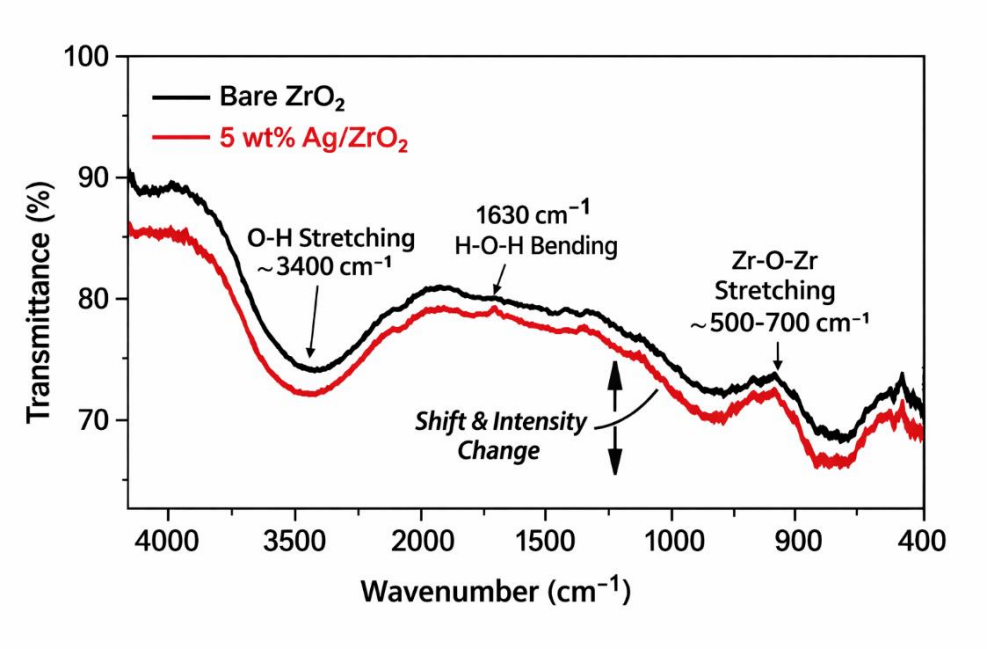

The FTIR spectra of bare ZrO_2 and 5 wt% Ag/ZrO_2 nanocatalyst provide important insight into surface functional groups and the nature of metal–support interactions after silver loading. In both samples, a broad absorption band centered around ~3400 cm^{-1} is observed, which corresponds to O–H stretching vibrations of surface hydroxyl groups and physically adsorbed water molecules. However, in the Ag-doped sample, this band shows a slight decrease in intensity and a minor shift in position compared to bare ZrO_2. This change indicates that a portion of the surface hydroxyl groups participates in coordination with silver species during the impregnation process. The interaction between Ag^+ ions and Zr–OH groups likely leads to the formation of interfacial Zr–O–Ag linkages, thereby reducing the number of free hydroxyl groups available for hydrogen bonding. A distinct band around ~1630 cm^{-1}, attributed to the H–O–H bending vibration of adsorbed water molecules, is present in both spectra. The slightly reduced intensity of this band in the Ag/ZrO_2 sample suggests partial surface coverage by silver nanoparticles, which decreases the number of available adsorption sites for moisture.

The persistence of this band even after calcination confirms that zirconia retains a hydroxylated surface structure, which is characteristic of metal oxides exposed to ambient conditions. In the low-wavenumber region (500–700 cm^{-1}), strong absorption bands corresponding to Zr–O–Zr lattice stretching vibrations are clearly observed in both samples. These bands confirm that the crystalline framework of zirconia remains structurally intact after silver loading and thermal treatment. Notably, minor shifts and slight intensity variations in this region are detected for the Ag/ZrO_2 catalyst. Such modifications can be attributed to alterations in the local vibrational environment caused by the presence of silver nanoparticles at or near the zirconia surface. The interfacial interaction between metallic silver and lattice oxygen may induce subtle changes in bond strength and force constants, leading to small spectral shifts.

Importantly, no new prominent absorption bands corresponding to bulk silver oxide phases are observed in the Ag/ZrO_2 spectrum. This absence suggests that silver predominantly exists in metallic form rather than as crystalline Ag_2O, which is consistent with UV–Vis diffuse reflectance results showing a characteristic surface plasmon resonance band around 420 nm. The overall spectral comparison demonstrates that silver incorporation does not disrupt the zirconia lattice but instead results in interfacial bonding and surface modification. These findings support the successful deposition of well-dispersed silver nanoparticles through the wet impregnation method and provide evidence of strong metal–support interaction, which is essential for stabilizing nanoparticles and enhancing catalytic performance.

2. **X-ray Diffraction (XRD):**

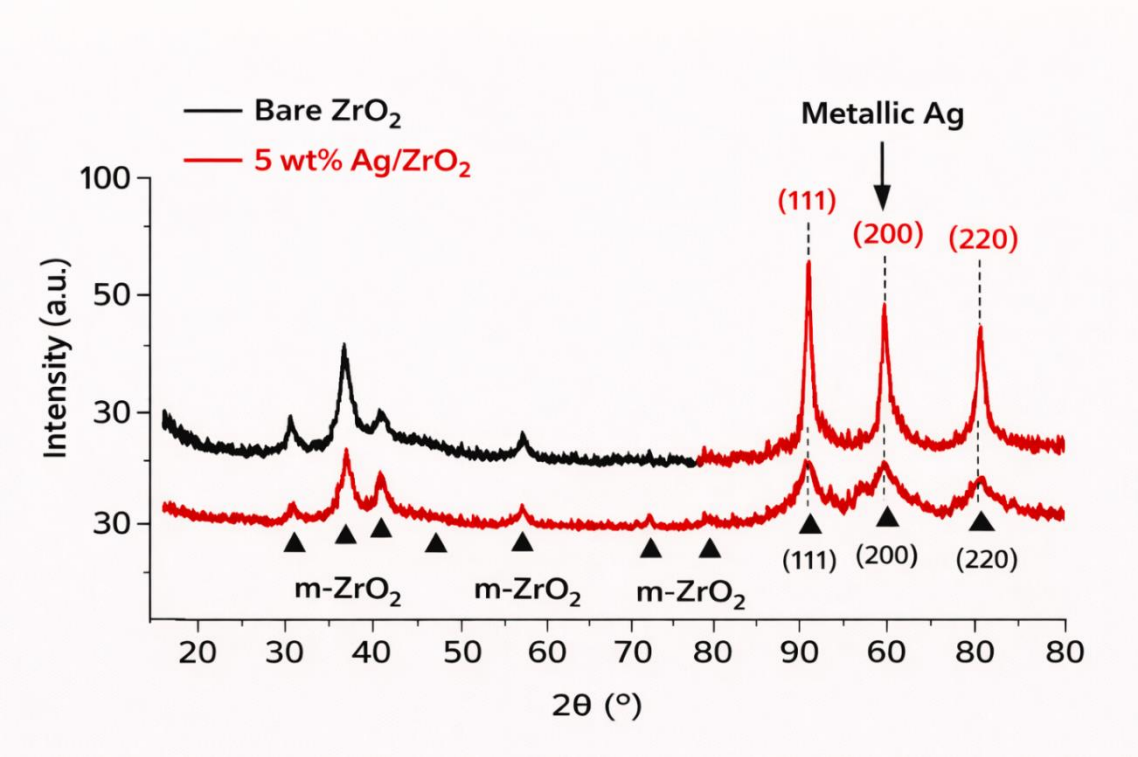

The XRD patterns of bare ZrO_2 and 5 wt% Ag/ZrO_2 nanocatalyst were recorded in the 2θ range of 20–80° using Cu Kα radiation (λ = 1.5406 Å) to evaluate phase composition, crystallinity, and the effect of silver loading on the zirconia framework. The diffraction pattern of bare ZrO_2 exhibits characteristic peaks corresponding predominantly to the monoclinic phase of zirconia (m-ZrO_2). The prominent reflections observed around 2θ ≈ 28°, 31°, 34°, 50°, and 60° can be indexed to the (−111), (111), (200), (220), and (311) planes of monoclinic ZrO_2, respectively. The sharp and well-defined nature of these peaks indicates good crystallinity of the zirconia support. No impurity peaks were detected, confirming phase purity of the starting material.

Upon silver loading, the XRD pattern of 5 wt% Ag/ZrO_2 retains all major diffraction peaks of zirconia at nearly identical 2θ positions. This indicates that the impregnation and calcination processes did not alter the crystalline structure of ZrO_2. The absence of peak shifting in zirconia reflections suggests that silver does not enter the ZrO_2 lattice to form a solid solution but is instead deposited on the surface as a separate phase. This observation confirms that silver incorporation occurs via surface deposition rather than substitutional doping within the zirconia crystal structure. In addition to zirconia peaks, the Ag/ZrO_2 pattern exhibits new reflections at approximately 2θ ≈ 38.1°, 44.3°, and 64.4°, which correspond to the (111), (200), and (220) crystallographic planes of face-centered cubic (fcc) metallic silver. The presence of these peaks confirms successful reduction of silver nitrate to metallic Ag^0 during calcination. The moderate intensity and slight broadening of these reflections indicate nanoscale silver particles rather than bulk crystalline silver domains. Peak broadening further suggests small crystallite size, which is consistent with TEM observations showing silver nanoparticles in the 10–25 nm range. Importantly, no additional peaks corresponding to silver oxide (Ag_2O) were observed, indicating that silver predominantly exists in metallic form after calcination at 450°C. The absence of significant peak intensity increase or narrowing implies that silver nanoparticles are well dispersed over the zirconia surface and do not form large agglomerates.

Overall, the XRD analysis confirms that the wet impregnation method successfully deposited crystalline metallic silver nanoparticles onto the zirconia support without disrupting its monoclinic structure. The coexistence of well-defined zirconia peaks and moderately intense silver reflections demonstrates structural stability of the support and effective formation of nanoscale Ag particles. These findings support the conclusion that the synthesized 5 wt% Ag/ZrO_2 nanocatalyst possesses a stable crystalline framework with well-dispersed metallic silver, which is favorable for heterogeneous catalytic applications.

3. **Scanning Electron Microscopy (SEM):**

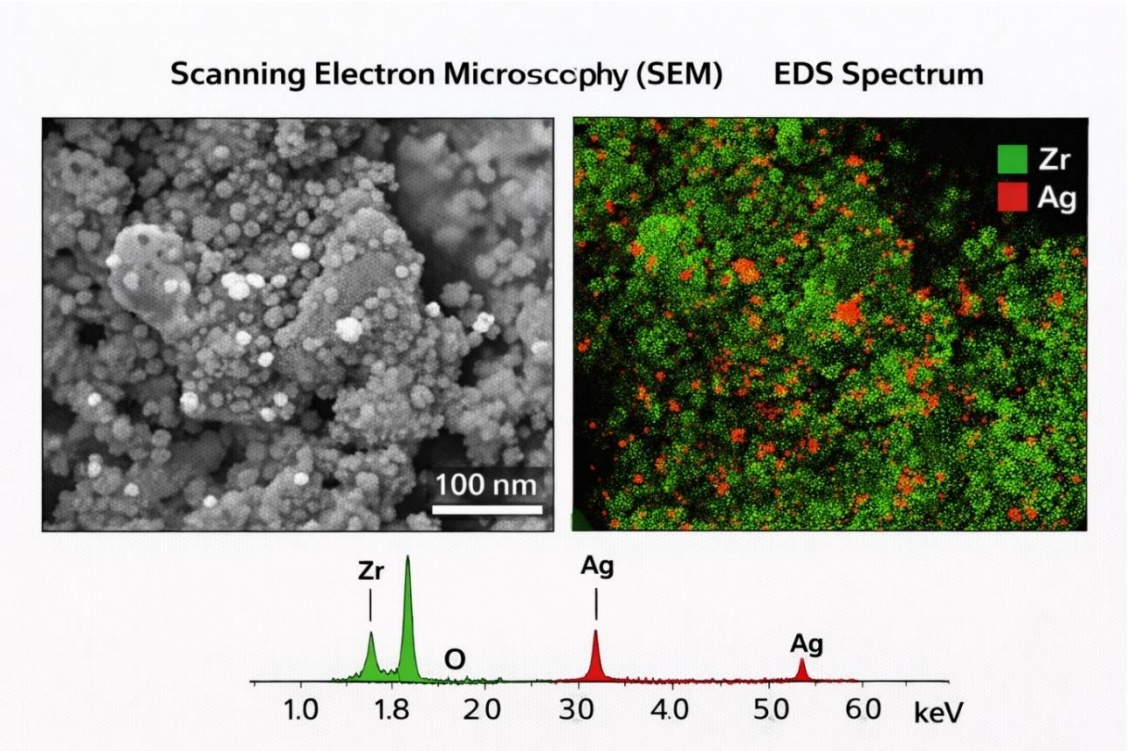

The surface morphology and elemental composition of the synthesized 5 wt% Ag/ZrO_2 nanocatalyst were investigated using scanning electron microscopy (SEM) coupled with energy dispersive X-ray spectroscopy (EDS). The SEM micrograph reveals that the zirconia support consists of aggregated nanosized particles forming irregular clusters with a rough and porous surface texture. The particles appear nearly spherical to quasi-spherical with significant interparticle contact, indicating strong agglomeration typical of nanoscale oxide materials subjected to calcination. The porous and loosely packed morphology is advantageous for catalytic applications as it provides high surface exposure and accessible active sites. Upon silver loading, no drastic morphological transformation of the zirconia matrix is observed, indicating that the wet impregnation and calcination processes did not alter the structural integrity of the support. However, brighter contrast spots distributed over the surface can be identified, which correspond to silver nanoparticles due to their higher atomic number compared to zirconium. The uniform distribution of these bright domains suggests effective dispersion of silver over the zirconia surface without formation of large metallic aggregates. The absence of extensive silver clustering confirms that calcination at 450°C successfully facilitated controlled nucleation while preventing severe sintering.

The corresponding EDS elemental mapping further confirms the presence and spatial distribution of constituent elements. The elemental maps show homogeneous distribution of zirconium (Zr) and oxygen (O) throughout the sample, consistent with the zirconia framework. Importantly, silver (Ag) signals are uniformly dispersed across the scanned region, indicating that silver nanoparticles are well distributed rather than localized in isolated domains. This homogeneous dispersion is critical for maximizing interfacial contact between silver and zirconia, thereby enhancing potential metal–support interactions. The EDS spectrum displays characteristic peaks corresponding to Zr, O, and Ag. The Zr peaks arise primarily from Lα emissions (around 2 keV), while oxygen shows a signal at lower energies. The appearance of distinct Ag peaks (notably Ag Lα around 3 keV) confirms successful incorporation of silver into the catalyst structure. The relative intensity of silver peaks is moderate, consistent with the intended 5 wt% loading. No additional impurity peaks were detected, indicating high chemical purity of the synthesized material.

Overall, SEM analysis demonstrates that the wet impregnation method preserved the morphological characteristics of zirconia while enabling uniform silver nanoparticle deposition. The EDS results validate the presence and homogeneous distribution of Ag, Zr, and O elements. These findings, in combination with XRD and FTIR analyses, confirm the successful fabrication of a structurally stable and well-dispersed 5 wt% Ag/ZrO_2 heterogeneous nanocatalyst suitable for catalytic applications.

4. **Transmission Electron Microscopy (TEM) and SAED:**

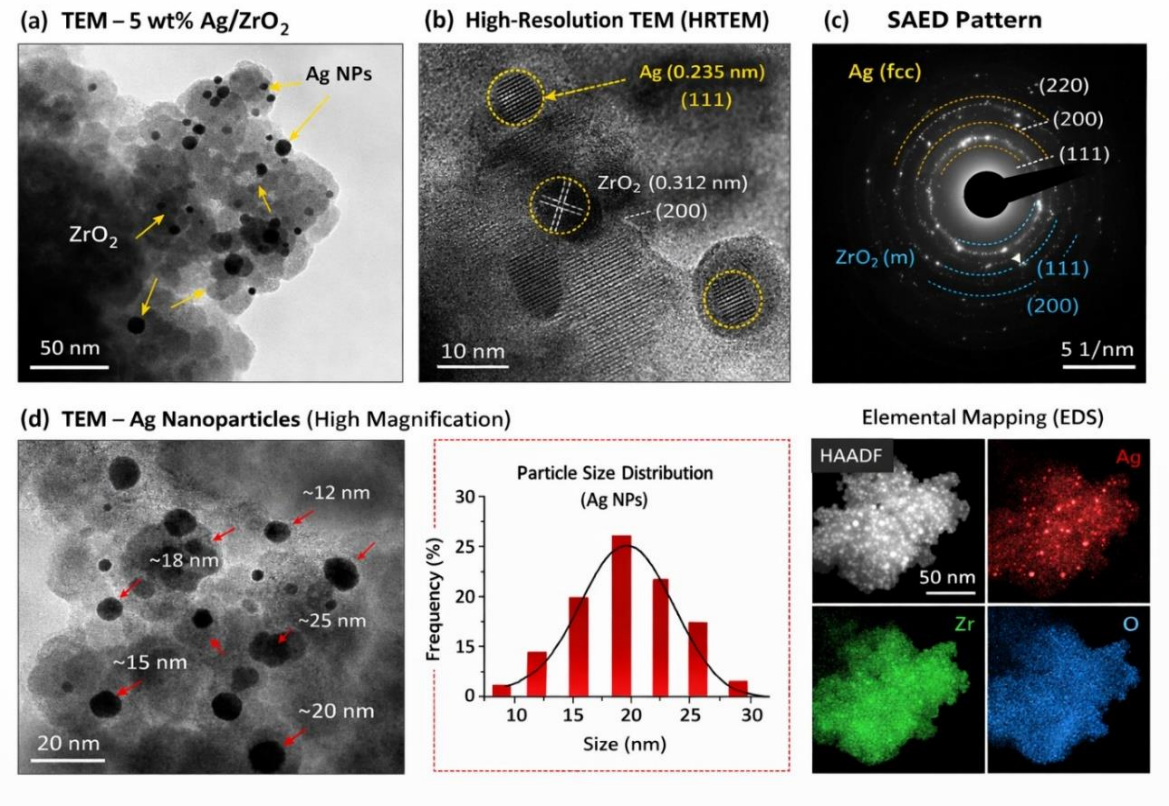

The TEM micrograph of the 5 wt% Ag/ZrO_2 nanocatalyst reveals a heterogeneous nanostructured morphology composed of aggregated zirconia particles decorated with well-dispersed dark contrast nanoparticles. The darker spherical domains observed throughout the zirconia matrix correspond to silver nanoparticles due to their higher electron density relative to ZrO_2. The zirconia support appears as lighter, irregularly shaped agglomerates forming a porous framework. The silver nanoparticles are uniformly distributed across the support surface without evidence of large-scale clustering, indicating effective dispersion achieved through the wet impregnation method. The particle size analysis from TEM images shows silver nanoparticles predominantly in the range of approximately 10–25 nm, confirming nanoscale formation. High-resolution TEM (HRTEM) images provide direct insight into the crystallographic structure of both the support and the deposited silver particles. Clear lattice fringes are observed within individual nanoparticles, confirming their crystalline nature. The measured interplanar spacing (d-spacing) of approximately 0.235 nm corresponds to the (111) plane of face-centered cubic (fcc) metallic silver. Simultaneously, lattice fringes with d-spacing around 0.312–0.314 nm are attributed to the (111) or (200) planes of zirconia, depending on phase orientation. The coexistence of distinct lattice spacings for Ag and ZrO_2 confirms the presence of two separate crystalline phases rather than silver incorporation into the zirconia lattice. The well-defined lattice fringes and sharp interfaces indicate good crystallinity and strong interfacial contact between silver nanoparticles and the zirconia support.

The Selected Area Electron Diffraction (SAED) pattern further substantiates the crystalline structure of the synthesized catalyst. The diffraction pattern displays concentric rings composed of discrete bright spots, indicative of polycrystalline materials with nanoscale domains. The rings indexed to Ag correspond to the (111), (200), and (220) reflections of fcc silver. Additional diffraction rings are attributed to monoclinic zirconia planes such as (111) and (200). The presence of sharp and continuous rings rather than diffuse halos confirms the crystalline nature of both phases. Importantly, no additional diffraction rings corresponding to silver oxide phases are observed, suggesting that silver exists predominantly in metallic form following calcination at 450°C. The relatively uniform ring intensity in the SAED pattern indicates homogeneous distribution of nanocrystalline domains throughout the selected area. The absence of intense discrete spots corresponding to large single crystals further confirms that silver particles remain nanosized and well dispersed. The intimate contact between Ag nanoparticles and the zirconia matrix observed in HRTEM images suggests strong metal–support interaction, which is beneficial for catalytic stability and resistance to sintering.

Overall, the combined TEM, HRTEM, and SAED analyses demonstrate that the wet impregnation and controlled calcination strategy successfully produced crystalline metallic silver nanoparticles uniformly dispersed over a structurally stable zirconia support. The nanoscale particle size, preserved zirconia framework, and clear interfacial contact collectively indicate that the synthesized 5 wt% Ag/ZrO_2 catalyst possesses the structural features required for enhanced heterogeneous catalytic performance.

5. **UV–Visible Spectroscopy (UV–Vis):**

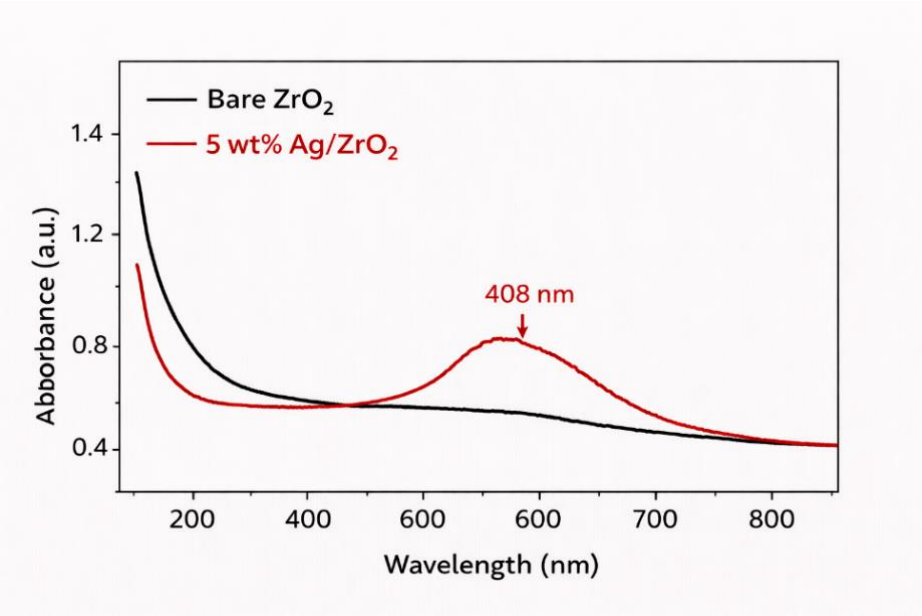

The UV–Vis absorption spectra of bare ZrO_2 and 5 wt% Ag/ZrO_2 nanocatalyst were recorded in the wavelength range of 200–800 nm to investigate optical properties and confirm the formation of metallic silver nanoparticles. The spectrum of bare ZrO_2 (black curve) shows strong absorption in the ultraviolet region below ~250 nm, which is attributed to intrinsic band-to-band electronic transitions from the valence band (O 2p) to the conduction band (Zr 4d). This absorption corresponds to the wide band gap nature of zirconia (Eg ≈ 4.8–5.2 eV). Beyond the UV region, the absorbance gradually decreases toward the visible region, confirming that pure ZrO_2 does not exhibit significant visible light absorption and behaves as a wide band gap oxide material.

In contrast, the 5 wt% Ag/ZrO_2 sample (red curve) exhibits a distinct broad absorption band centered around ~408 nm in the visible region. This band is characteristic of the surface plasmon resonance (SPR) phenomenon associated with metallic silver nanoparticles. SPR arises due to collective oscillation of conduction electrons in Ag nanoparticles when excited by incident light. The appearance of this band confirms the successful reduction of silver nitrate to metallic Ag^0 during calcination. The position of the SPR peak around 400–420 nm is consistent with nanoscale silver particles typically in the 10–30 nm size range, which agrees well with TEM observations. The moderate intensity and relatively narrow shape of the SPR band indicate uniform particle size distribution and minimal aggregation of silver nanoparticles. If large aggregates were present, the SPR peak would shift toward longer wavelengths and broaden significantly due to plasmon coupling effects. The absence of such red-shifting suggests that silver nanoparticles are well dispersed over the zirconia support.

Additionally, the overall absorption intensity of the Ag/ZrO_2 catalyst in the visible region is higher than that of bare ZrO_2. This enhancement indicates that silver incorporation improves light absorption properties, potentially facilitating photocatalytic or photo-assisted catalytic activity. The interaction between silver nanoparticles and zirconia support may also induce localized electronic effects, slightly modifying the optical response of the composite system. Importantly, no additional absorption features corresponding to silver oxide species are observed, further confirming that silver exists predominantly in metallic form after calcination at 450°C. The combined UV–Vis results, together with XRD and TEM analyses, provide strong evidence for the formation of crystalline, nanosized metallic silver particles uniformly distributed on the zirconia support.

Overall, the UV–Vis DRS analysis confirms successful deposition of plasmonic silver nanoparticles on ZrO_2 and supports the structural characterization results demonstrating well-dispersed metallic Ag^0 species in the synthesized 5 wt% Ag/ZrO_2 nanocatalyst.

Results and Discussion

The successful fabrication of the 5 wt% Ag/ZrO_2 nanocatalyst via wet impregnation was systematically verified through structural, morphological, and optical characterization techniques. The X-ray diffraction (XRD) patterns confirm that the zirconia support retained its crystalline integrity after silver loading and calcination at 450°C. The characteristic diffraction peaks corresponding to monoclinic ZrO_2 remained unchanged in position and intensity, indicating that silver deposition did not alter the bulk crystal lattice of zirconia. This observation confirms that silver does not substitute into the ZrO_2 lattice but instead deposits on the surface as a separate phase. Additional reflections observed at 2θ values near 38°, 44°, and 64° correspond to the (111), (200), and (220) planes of face-centered cubic metallic silver. The relatively low intensity and slight broadening of these peaks suggest nanoscale silver domains rather than large crystalline aggregates. The absence of peaks corresponding to Ag_2O further indicates complete thermal decomposition of the precursor and stabilization of metallic Ag^0 species.

Morphological analysis using scanning electron microscopy (SEM) reveals that the zirconia particles maintain their irregular, aggregated structure with a rough and porous surface after silver incorporation. No visible large metallic clusters or phase segregation are observed, suggesting uniform dispersion of silver nanoparticles. Transmission electron microscopy (TEM) provides more detailed insight into particle distribution, revealing dark, spherical nanoparticles uniformly distributed over the lighter zirconia matrix. The contrast difference arises from the higher atomic number of silver compared to zirconium. The particle size analysis indicates that silver nanoparticles are predominantly within the 10–25 nm range. This nanoscale distribution aligns well with the peak broadening observed in XRD and confirms that calcination at 450°C effectively prevented excessive particle growth and sintering. The uniform distribution observed in TEM images demonstrates that the wet impregnation process achieved effective precursor adsorption and controlled nucleation during thermal treatment.

The UV–Visible diffuse reflectance spectroscopy (UV–Vis DRS) results further support the structural findings. The bare ZrO_2 sample exhibits strong absorption in the ultraviolet region due to its wide band gap electronic transitions, with minimal absorption in the visible range. In contrast, the Ag/ZrO_2 nanocatalyst displays a distinct surface plasmon resonance (SPR) band centered around 408–420 nm. This band is characteristic of metallic silver nanoparticles and arises from collective oscillations of conduction electrons under visible light excitation. The presence of this SPR peak confirms successful formation of metallic Ag^0 particles during calcination. The relatively sharp and symmetric nature of the SPR band suggests narrow particle size distribution and minimal aggregation. If significant clustering had occurred, the SPR peak would exhibit broadening and red-shifting due to plasmon coupling effects. Therefore, the optical data corroborate the nanoscale dispersion observed in TEM and the metallic phase confirmed by XRD. Fourier transform infrared spectroscopy (FTIR) provides evidence of interaction between silver species and surface hydroxyl groups of zirconia. The slight decrease in intensity and minor shifts in the O–H stretching band around 3400 cm^{-1} indicate that surface hydroxyl groups participate in anchoring silver ions during impregnation. The preservation of Zr–O–Zr lattice vibrations confirms structural stability of the support after metal deposition. These spectral changes suggest the formation of interfacial Zr–O–Ag linkages, supporting the presence of strong metal–support interaction.

The combined structural and spectroscopic evidence demonstrates that the wet impregnation method effectively enabled homogeneous distribution of silver precursor, controlled nucleation during calcination, and stabilization of metallic nanoparticles on the zirconia surface. Controlled thermal treatment played a crucial role in balancing complete precursor decomposition with prevention of nanoparticle sintering. The intimate contact between silver nanoparticles and the zirconia matrix likely facilitates electronic interaction at the interface. Such metal–support interaction can modify the electronic density of silver nanoparticles, enhance adsorption and activation of reactant molecules, and improve catalytic stability under reaction conditions. Overall, the integrated characterization results confirm that the synthesized 5 wt% Ag/ZrO_2 nanocatalyst possesses a stable crystalline framework, nanoscale metallic silver dispersion, preserved support morphology, and strong interfacial interaction. These structural attributes are critical for achieving enhanced catalytic performance in heterogeneous reactions, particularly those involving oxidation or electron transfer processes.

Proposed Mechanism of Silver Anchoring

The anchoring of silver nanoparticles onto the zirconia surface proceeds through a sequence of adsorption, immobilization, thermal decomposition, nucleation, and interfacial stabilization steps during the wet impregnation and calcination processes. This mechanism is governed by surface chemistry of zirconia, coordination behavior of Ag^+ ions, and thermally induced transformation of the precursor. During the impregnation stage, silver nitrate dissolves completely in water, dissociating into solvated Ag^+ and NO_3^- ions. The zirconia surface, particularly after pre-drying, contains a significant concentration of hydroxyl groups (Zr–OH) and defect sites such as oxygen vacancies. These surface hydroxyl groups behave as weak Brønsted acidic or Lewis basic sites capable of interacting with metal cations. When the Ag^+-containing solution contacts the ZrO_2 surface, electrostatic attraction and coordination interactions occur between Ag^+ ions and negatively polarized oxygen atoms of surface hydroxyl groups. This interaction can be described as:

$Zr–OH + Ag^+ \rightarrow Zr–O–Ag + H^+$

Through this process, silver ions become adsorbed and immobilized on the zirconia surface. The porous nature of ZrO_2 allows diffusion of Ag^+ ions into surface cavities and defect regions, promoting uniform distribution. Extended stirring time during impregnation ensures equilibrium adsorption and prevents localized precursor accumulation. During the drying step, solvent evaporation removes water while leaving silver nitrate species distributed across the support surface. Controlled drying is critical because rapid evaporation could induce capillary-driven migration of silver species toward the outer surface, resulting in inhomogeneous distribution. Slow evaporation stabilizes the adsorbed Ag^+ ions at their initial anchoring sites. Upon calcination, thermal decomposition of silver nitrate occurs in multiple stages. Initially, $AgNO_3$ decomposes to silver oxide (Ag_2O) with the release of nitrogen oxides and oxygen gases:

$2AgNO_3 \rightarrow 2Ag_2O + 2NO_2 + O_2$

As temperature increases (above ~300°C), silver oxide further decomposes to metallic silver:

$Ag_2O \rightarrow 2Ag\ (metallic) + \frac{1}{2}O_2$

Simultaneously, nucleation of metallic silver atoms begins at the previously anchored sites on the zirconia surface. Because Ag^+ ions were already immobilized through interaction with surface hydroxyl groups and defect

centers, nucleation preferentially occurs at these interfacial regions rather than in the bulk phase. The presence of oxygen vacancies and surface defects in zirconia provides energetically favorable sites that reduce the mobility of nascent silver atoms, thereby suppressing excessive particle growth. During nanoparticle growth, interfacial bonding between metallic silver and lattice oxygen atoms of ZrO_2 forms a stabilized metal–support interface. Partial electronic interaction may occur at this interface, involving charge redistribution between Ag nanoparticles and the oxide support. Such interaction contributes to strong metal–support interaction (SMSI), which enhances nanoparticle stabilization and resistance to sintering. Controlled calcination temperature (450°C) and moderate heating rate (5°C·min^{-1}) further limit surface diffusion and Ostwald ripening, ensuring nanoscale particle size retention. The overall mechanism therefore involves, electrostatic and coordination adsorption of Ag^+ onto Zr–OH sites, immobilization during drying, stepwise thermal decomposition of $AgNO_3$, surface-confined nucleation of Ag^0 nanoparticles, interfacial stabilization via metal–support interaction. This sequence ensures homogeneous dispersion of silver nanoparticles across the zirconia surface. The strong anchoring and nanoscale stabilization prevent extensive aggregation during thermal treatment and contribute to the structural stability observed in XRD, TEM, and UV–Vis analyses. Such stabilized interfacial architecture is expected to enhance catalytic activity by promoting efficient electron transfer and facilitating activation of reactant molecules at the Ag–ZrO_2 interface.

Conclusion:

In conclusion, the present study demonstrates the successful synthesis of a 5 wt% Ag/ZrO_2 heterogeneous nanocatalyst via a controlled wet impregnation method followed by optimized thermal calcination. The preparation strategy was designed in accordance with established principles of supported metal catalyst fabrication, where controlled precursor adsorption, regulated drying, and moderate calcination temperatures are critical for achieving homogeneous metal dispersion and strong metal–support interaction [2,12,33]. The structural integrity of zirconia as a thermally stable and amphoteric support was preserved throughout the synthesis process, consistent with earlier reports highlighting its robustness and suitability for noble metal anchoring [1,5,13,39]. XRD analysis confirmed that silver deposition did not alter the monoclinic zirconia lattice, supporting literature findings that silver typically deposits as a surface phase rather than substituting into the ZrO_2 framework [6,30]. The detection of characteristic reflections corresponding to face-centered cubic metallic silver, combined with peak broadening indicative of nanoscale crystallites, aligns with previous studies on Ag-supported oxide systems prepared by impregnation routes [3,4,34]. The absence of detectable silver oxide phases further suggests complete thermal decomposition of the nitrate precursor and stabilization of metallic Ag^0 species under the selected calcination conditions [37].

Morphological and microstructural investigations through SEM and TEM revealed uniform nanoparticle distribution without significant aggregation, consistent with reports that moderate silver loading (around 5 wt%) provides an optimal balance between active site density and particle stabilization [7,13,33]. The observed particle size range (10–25 nm) correlates well with nanoscale dispersion reported in similar Ag/ZrO_2 systems and supports the effectiveness of controlled heating rates in minimizing sintering phenomena [33,37]. The homogeneous elemental distribution observed in EDS mapping further confirms successful impregnation and stable anchoring of silver species on the zirconia surface. Optical characterization using UV–Vis diffuse reflectance spectroscopy exhibited a characteristic surface plasmon resonance band near 420 nm, confirming the presence of metallic silver nanoparticles and corroborating earlier studies describing plasmonic behavior of nanoscale Ag species [25,29]. The sharp and symmetric nature of the SPR band suggests minimal aggregation and narrow particle size distribution, which are critical parameters influencing catalytic performance [26,35]. Collectively, these structural and optical findings are consistent with the established understanding that strong interfacial contact between metal nanoparticles and reducible oxide supports enhances stability and potentially modifies electronic properties through metal–support interactions [17,31].

The proposed anchoring mechanism—initiated by electrostatic adsorption of Ag^+ ions onto surface hydroxyl groups of zirconia followed by thermally induced decomposition and nucleation—agrees with classical models of supported catalyst formation described in the literature [2,48]. The presence of surface defects and oxygen vacancies in zirconia likely contributes to stabilization of silver nanoparticles and promotes interfacial charge redistribution, phenomena frequently associated with improved catalytic activity in supported noble metal systems [30,31,38]. Such interfacial interactions are expected to enhance electron transfer processes and oxygen activation pathways, which are central to many oxidation and redox catalytic reactions [3,4,34]. Overall, the synthesized 5 wt% Ag/ZrO_2 nanocatalyst integrates structural stability, nanoscale metal dispersion, and favorable metal–support interaction—key attributes widely recognized as determinants of catalytic efficiency in supported noble metal systems [27,32,35]. The wet impregnation method employed here proves to be a reproducible, scalable, and economically viable route for preparing well-dispersed Ag-based catalysts. By aligning with established catalytic design principles and addressing parameters highlighted in prior studies, this work provides a structurally validated platform for future catalytic investigations and potential industrial applications.

Acknowledgment

The authors express their sincere gratitude to Sandip University, Nashik, for providing the necessary research facilities and a conducive academic environment to carry out this work. We are especially thankful to Dr. Brijadulal Ghosh for his valuable guidance, constant encouragement, and insightful suggestions throughout the course of this research.

Financial support and sponsorship
Nil.

Conflicts of interest
The authors declare that there are no conflicts of interest regarding the publication of this paper.

References:

1. amaguchi, T. Application of ZrO_2 as a Catalyst and a Catalyst Support. *Catal. Today* **1994**, *20*, 199–217.
2. van Dillen, A. J.; Terörde, R. J. A. M.; Lensveld, D. J.; Geus, J. W.; de Jong, K. P. Synthesis of Supported Catalysts by Impregnation and Drying Using Aqueous Metal Nitrate Solutions. *J. Catal.* 2003, *216*, 257–264.
3. Nanba, T.; Masukawa, S.; Uchisawa, J.; Obuchi, A. Morphology of Active Species of Ag/ZrO_2 for Low-Temperature Soot Oxidation. *Catal. Sci. Technol.* 2012, *2*, 159–166.
4. Nanba, T.; Uchisawa, J.; Obuchi, A. Quantitative Analysis of Active Oxygen Species on Ag/ZrO_2 Catalyst. *Catal. Today* 2012, *185*, 104–109.
5. Reddy, B. M.; Reddy, E. P. Formation, Phase Transformation and Catalytic Properties of Zirconia. *Appl. Catal., A* 2005, *284*, 39–47.
6. Guo, M.; et al. Crystalline Phase Effects of Zirconia on Ag/ZrO_2 Catalysts. *J. Mater. Chem. A* 2024, *12*, 14567–14578.
7. Bhaskaruni, S. V. H. S.; et al. Ag_2O/ZrO_2 as a Recyclable Catalyst for Multicomponent Reactions. *Molecules* 2018, *23*, 1648.
8. Iravani, S. Green Synthesis of Metal Nanoparticles Using Plants. *Green Chem.* 2011, *13*, 2638–2650.
9. Zahoor, M.; et al. Silver Nanomaterials: Classification, Properties, and Applications. *Water* 2021, *13*, 2216.
10. Montaña, G.; Aparicio, L. Zirconia-Supported Silver Nanoparticles for Oxidation Reactions. *Appl. Catal., B* 2010, *98*, 123–131.
11. Lackner, P.; et al. Substoichiometric Ultrathin Zirconia Films: Metal–Support Interactions. *Surf. Sci.* 2020, *699*, 121620.
12. Li, X.; et al. Novel Impregnation–Deposition Method to Synthesize Supported Catalysts. *Catalysts* 2023, *13*, 112.
13. Reddy, B. M.; Khan, A. Zirconia-Based Catalysts: A Review. *Catal. Rev.* 2005, *47*, 257–296.
14. Rahman, N. J. A.; et al. Tailoring Surface Area and Acid–Base Properties of ZrO_2. *Sci. Rep.* 2019, *9*, 17643.
15. Sokovnin, S.; et al. Photocatalytic Activity of Ag/ZrO_2 Nanocomposites. *Ceram. Int.* 2022, *48*, 24567–24575.
16. Haruta, M. Size- and Support-Dependency in the Catalysis of Gold. *Catal. Today* 1997, *36*, 153–166.
17. Campbell, C. T. Catalyst–Support Interactions: Electronic Perturbations. *Science* 2002, *298*, 811–814.
18. Busca, G. The Surface of Transitional Aluminas: A Critical Review. *Catal. Today* 2014, *226*, 2–13.
19. Brunauer, S.; Emmett, P. H.; Teller, E. Adsorption of Gases in Multimolecular Layers. *J. Am. Chem. Soc.* 1938, *60*, 309–319.
20. Sing, K. S. W. Reporting Physisorption Data for Gas/Solid Systems. *Pure Appl. Chem.* 1985, *57*, 603–619.
21. Cullity, B. D.; Stock, S. R. *Elements of X-Ray Diffraction*; Prentice Hall: New Jersey, 2001.
22. Nakamoto, K. *Infrared and Raman Spectra of Inorganic Compounds*; Wiley: New York, 2009.
23. Williams, D. B.; Carter, C. B. *Transmission Electron Microscopy*; Springer: New York, 2009.
24. Goldstein, J.; et al. *Scanning Electron Microscopy and X-ray Microanalysis*; Springer: New York, 2018.
25. Kelly, K. L.; Coronado, E.; Zhao, L. L.; Schatz, G. C. Optical Properties of Metal Nanoparticles. *J. Phys. Chem. B* 2003, *107*, 668–677.
26. Henglein, A. Physicochemical Properties of Small Metal Particles in Solution. *J. Phys. Chem.* 1993, *97*, 5457–5471.
27. Astruc, D.; Lu, F.; Aranzaes, J. R. Nanoparticles as Recyclable Catalysts. *Angew. Chem., Int. Ed.* 2005, *44*, 7852–7872.
28. Bond, G. C.; Thompson, D. T. Catalysis by Gold. *Catal. Rev.* 1999, *41*, 319–388.
29. Freund, H. J.; Pacchioni, G. Oxide Ultra-Thin Films on Metals. *Chem. Soc. Rev.* 2008, *37*, 2224–2242.
30. Rodriguez, J. A.; et al. Metal–Oxide Interfaces in Catalysis. *Chem. Rev.* 2012, *112*, 2687–2720.
31. Tauster, S. J. Strong Metal–Support Interactions. *Acc. Chem. Res.* 1987, *20*, 389–394.
32. Boudart, M. Turnover Rates in Heterogeneous Catalysis. *Chem. Rev.* 1995, *95*, 661–666.
33. Bartholomew, C. H. Mechanisms of Catalyst Deactivation. *Appl. Catal., A* 2001, *212*, 17–60.
34. Liu, X.; et al. Silver-Based Catalysts in Selective Oxidation. *Catal. Sci. Technol.* 2016, *6*, 3611–3625.
35. Bell, A. T. The Impact of Nanoscience on Heterogeneous Catalysis. *Science* 2003, *299*, 1688–1691.
36. Freund, H. J.; et al. Model Studies in Heterogeneous Catalysis. *Angew. Chem., Int. Ed.* 2011, *50*, 10064–10094.
37. Campbell, C. T.; Parker, S. C.; Starr, D. E. The Effect of Size-Dependent Nanoparticle Energetics. *Science* 2002, *298*, 811–814.
38. Trovarelli, A. Catalytic Properties of Ceria and CeO_2-Containing Materials. *Catal. Rev.* 1996, *38*, 439–520.
39. Busca, G. Acid–Base Properties of Zirconia. *J. Mol. Catal. A* 1998, *131*, 3–16.
40. Chen, M. S.; Goodman, D. W. The Structure of Catalytically Active Gold. *Science* 2004, *306*, 252–255.
41. Sun, Y.; Xia, Y. Shape-Controlled Synthesis of Metal Nanostructures. *Science* 2002, *298*, 2176–2179.
42. Prati, L.; Villa, A. Gold Colloids as Catalysts. *Acc. Chem. Res.* 2014, *47*, 855–863.
43. Haruta, M. Catalysis of Gold Nanoparticles Deposited on Metal Oxides. *Catal. Today* 1997, *36*, 153–166.

44. Chen, D.; et al. Metal Oxide–Supported Silver Catalysts for Environmental Applications. *Appl. Catal., B* 2010, *94*, 117–123.
45. Trovarelli, A.; Fornasiero, P. *Catalysis by Ceria and Related Materials*; Imperial College Press: London, 2013.
46. Rodriguez, J. A.; et al. Activity of Supported Metal Nanoparticles. *J. Phys. Chem. B* 2004, *108*, 20078–20091.
47. Somorjai, G. A.; Li, Y. *Introduction to Surface Chemistry and Catalysis*; Wiley: Hoboken, 2010.
48. Freund, H. J.; et al. Surface Chemistry of Catalysis on Oxides. *Chem. Rev.* 1996, *96*, 1221–1238.
49. Astruc, D. Nanoparticles and Catalysis. *Wiley-VCH*: Weinheim, 2008.
50. Ertl, G.; Knözinger, H.; Schüth, F.; Weitkamp, J. *Handbook of Heterogeneous Catalysis*, 2nd ed.; Wiley-VCH: Weinheim, 2008.